International Journal of Thermal Sciences 48 (2009) 2006–2012

Contents lists available at ScienceDirect

International Journal of Thermal Sciences

journal homepage: www.elsevier.com/locate/ijts

Conjugate fluid flow and kinetics modeling for heat exchanger fouling simulation

Maria Valeria De Bonis, Gianpaolo Ruocco*

DITEC, Università degli studi della Basilicata, Campus Macchia Romana, Potenza 85100, Italy

ARTICLE INFO

Article history:
Received 31 March 2008
Received in revised form
10 December 2008
Accepted 6 March 2009
Available online 11 April 2009

Keywords:
Heat exchanger
Fluid flow
Heat transfer
Mass transfer
Fouling kinetics

ABSTRACT

Thermal treatment of fluid foods represents a major unit operation in the food industry, to ensure the product's safety and quality features. But during the thermal treatments of such sensible fluids in common plate heat exchangers, food constituents such as proteins can be thermally damaged and precipitated to form fouling that greatly affect the treatment efficiency and alter the product's desired features.

Computational Fluid Dynamics simulations can then be successfully exploited, bringing forth temperature and velocity information that yield for deposit distributions when coupled to biochemical notations for thermal denaturation of fluid constituents.

The present work exploits such modeling for a single-channel heat exchanger during pasteurization of milk. The model enforces a conjugate system of differential equations to a heat exchanger's corrugated plate to combine flow, heat transfer and local transport of β-lactoglobulin. A preliminary computation has been performed that could be applied to geometry optimization (different corrugation shape and orientation) and for a variety of biochemically evolutive products.

1. Introduction

The increasing attention on safety and quality of medium and long time shelf-life has stimulated the application of various and optimized thermal treatments, in order to get flavor and nutritional values closer to those of untreated foods. For this very reason, thermal treatment of fluid foods is one of the most important unit operation in the dairy (milk) or fruit juices industry, to ensure microbial safety and extend storage. Energy delivery is a paramount parameter (through temperature) in controlling the alterations among the fluid constituents during its biochemical evolution, and must be coupled with time exposure, to quantify the energy intake. Therefore the temperature–time coupling is the most important feature to be optimized in this technology, but recently the attention has been drawn upon the management of the treatment device as well, as reviewed by Jun and Puri [6].

The device generally entitled to realize an indirect heating of fluid food is the Plate Heat Exchanger (PHE) (Fig. 1), which features a number of favorable aspects: flexibility to allow different fluid treatment, safety, high thermofluid efficiency, high turbulence to enhance heat transfer and low weight/surface ratio [11]. Nevertheless, during its working cycles, a PHE is subject to a complex phenomenon which causes undesired material accumulation (or fouling) along its working surfaces. Fouling formation and control is a common problem in process industries, causing an increase of capital costs, energy and maintenance time, and a loss of production, together with a meaningful environmental impact: fouling causes increased pressure drop, reduction of working efficiency through the reduction of the heat transfer, and increased downtime due to the frequent cleaning stage, with environmentally offensive chemicals, to ensure stable processing [1,2].

The biochemical fouling mechanism has been long studied specially for milk processing, and its reflected flow-dependent features have favored some complex analyses. As shown by de Jong et al. [12], Georgiadis et al. [3], Georgiadis and Macchietto [4] and Grijspeerdt et al. [5], the denaturation of the β-lactoglobulin (βLG) protein is responsible for fouling for thermal treatment close to 90 °C, while several additional parameters influencing such as milk composition, pH, plate geometry and entrained air.

The optimization of technological process and their operating conditions are nowadays looked upon with the aid of numerical modeling of transfer phenomena. Integration of governing Partial Differential Equations (PDEs) allows for a fundamental and quantitative way to understand complex phenomena which is complementary to the traditional approaches of theory and experiment. This approach is becoming increasingly widespread in basic research and advanced technological applications, cross cutting many scientific fields including biotechnology and food engineering. Again for the dairy industry, Georgiadis and Macchietto [4]

* Corresponding author.
E-mail address: gianpaolo.ruocco@unibas.it (G. Ruocco).

1290-0729/$ – see front matter © 2009 Elsevier Masson SAS. All rights reserved.
doi:10.1016/j.ijthermalsci.2009.03.010

Nomenclature

α	thermal diffusivity (m^2/s)
c	molar concentration (mol/m^3)
D	mass diffusivity (m^2/s)
K	reaction rate (1/s)
ν	kinematic viscosity (m^2/s)
p	pressure (Pa)
R	source term of reactions (kg/m^3 s)
Re	Reynolds number, based on channel height
ρ	density (kg/m^3)
t	time (s)
T	temperature (K)
v	velocity vector (m/s)

Subscripts

A	aggregated protein
D	denaturated unfolded protein
F	deposited protein
i,j	species
N	native protein
r	reaction
s	superficial
v	volumetric

proposed a mathematical model by integrating a PDEs plug-flow model with the heat convection along the flow direction and the effects of dispersion. Fouling is considered as mono-dimensional at steady state, and different heat exchanger configurations are compared by using a specific software to quantify the fouling distribution in the whole device. The deposit varies linearly with time, specially at the beginning of treatment, and is non-uniform in the different channels considered being more localized in the first flow passages, where temperature is higher. Nema and Datta [9] proposed a model to predict the fouling thickness and the milk outlet temperature in a helical triple tube heat exchanger. The fouling is controlled by temperature and shear stress on the surface of the heat exchanger. The milk outlet temperature was simulated, and the fouling thickness was determined based on the enthalpy balance and assuming a constant heat flux across the heat exchanger wall, but based on empirical considerations leading to a dimensionless fouling factor in the form of a Biot number. Then Jun and Puri [7] have employed a full two-dimensional Navier–Stokes formulation for the flow field, but again the use of a Biot number to calculate the overall heat transfer coefficient prevented a complete conjugate approach. Though still idealized (plates have no corrugations) they showed that the temperature distribution and related fouling could be predicted based on a complex combination of transport equations. A validation was also carried out, which compared favorably with tests, for several thermal and fluid flow conditions, confirming that the deposit is strongly dependent on operating conditions.

It should be insisted here that the complex combination of transport phenomena and technological aspects at hand suggests that the fouling must be retained in a conjugate framework: this means that the transfers of mass and heat are solved simultaneously in both solid (channel wall or fouling surface) and fluid phases, and are strongly coupled through deposition and properties variation due to velocity field and temperature. Therefore an innovative approach is to solve a model in which the mass and energy interface fluxes vary seamlessly in space and time as the solution of field variables, such as velocity. The transport equations contain the macroscopic term of convective transport and a source term allowing for the fouling creation, but the boundary conditions at the internal surfaces are independent on transfer coefficients or on the definition of boundary layers.

Computational Fluid Dynamics (CFD) can be enforced to solve governing PDEs. The detailed flow field study, coupled to the other transport notations, offers a potential of improved performance, better reliability, more confident scale-up, improved product consistency, and higher plant productivity. All these aspects give deeper understanding of what is happening in a particular process or system: it makes it possible to evaluate geometric changes, for example, with much less time and cost than would be involved in laboratory testing, it can answer many "what if" questions in a short time and, finally, it is particularly useful in simulating conditions where it is not possible to take detailed measurements.

In the present work the PDE problem, with the related biochemical notations, has been solved by using a commercial Finite Element solver [13] in order to determine the temperature distribution, the velocity profile and the distribution of the protein deposit. The model is the basis for more specialized computations aimed to minimize fouling, i.e. by modifying the fluid dynamics regime or corrugation shape and orientation. The application of the model could be beneficial to the food and biotechnology industry, suggesting the application of specific heat exchanger geometries for a specific product or process.

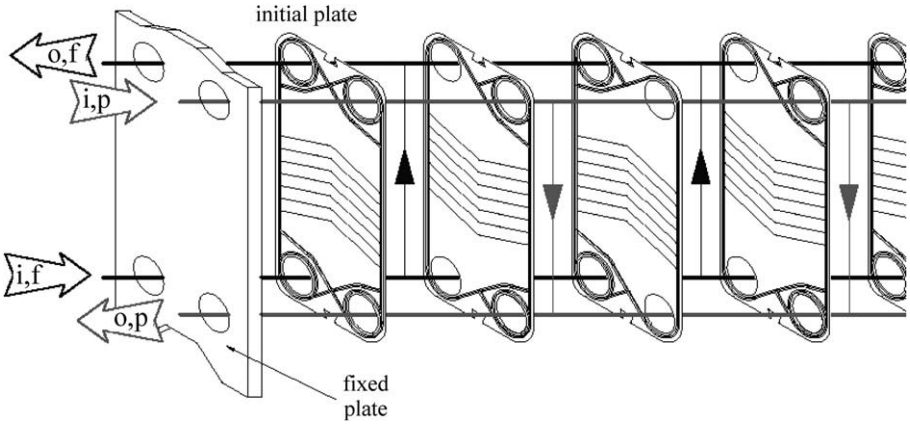

Fig. 1. The stacked PHE arrangement, with indication of streams. The product line with gray lines and arrows (p), and the auxiliary fluid (thermal carrier) with black lines and arrows (f) are reported, respectively, at inlet (i) and outlet (o).

2. Problem formulation

In the present work a pasteurization treatment of milk in the first channel passage of a PHE has been studied (Fig. 2A), to analyze the βLG's denaturation and subsequent aggregation and compare with the available literature findings. The transfer phenomena at hand are based on the βLG's local kinetics mechanisms and related time evolution, depending on the adopted thermal regime and flow geometry.

The subject control volume in Fig. 2B is formed by two AISI 4340 steel, 25-cm long and 1-mm thick, parallel plates. These form a 4 mm height channel; the inferior trapezoidal corrugations have long side, short side and height equal to 5, 1 and 3 mm, respectively, are spaced by 2 cm and are associated to specular superior vanes.

2.1. Driving assumptions

The following considerations have been adopted:

(1) The product flow is two-dimensional, in rectangular Cartesian coordinates, laminar and incompressible (negligible pressure work and kinetic energy), and with constant properties.
(2) The viscous heat dissipation is neglected.
(3) Due to the adopted flow regime, no body force is accounted for.
(4) Mass diffusivities of species have been computed by following Jun and Puri [7] specifications.

Furthermore, as the present work is focused on the evolution of βLG, it is suitable to include it in the CFD formalism. The Jun and Puri [7] version of the original reaction scheme by de Jong etal. [12] is adopted:

(1) Proteins react in both the bulk fluid and a thermal boundary layer. Native protein *N* is transformed to denaturated unfolded protein *D* by a first order reaction. The unfolded protein then reacts to give an aggregated protein *A* by a second order reaction.
(2) Mass transfer between the bulk and the thermal boundary layer takes place for each protein form.
(3) An aggregated protein *F* only fouls the channel wall. The rate of deposition is proportional to the concentration of protein *A* in the thermal boundary layer.
(4) The fouling resistance to heat transfer is proportional to the thickness of the deposit *F*.

This scheme can be summarized by the following reaction rate *R* scheme:

$$N \overset{R_{ND}}{\rightarrow} D \overset{R_{DA}}{\rightarrow} A \overset{R_{AF}}{\rightarrow} F \tag{1}$$

2.2. Governing equations

Combining this in a CFD framework, the standard unsteady-state governing Navier–Stokes, energy and mass conservation PDEs are enforced for the two-phase channel system, in conservative form and for primitive variables, to yield for velocity components, pressure, mass fractions distributions in the fluid phase, and temperature distribution in both phases and confining plates:

$$\nabla \cdot \mathbf{v} = 0 \tag{2}$$

where $\mathbf{v}$ is the milk velocity, null in the solid phase;

$$\frac{\partial \mathbf{v}}{\partial t} + \mathbf{v} \cdot \nabla \mathbf{v} + \frac{1}{\rho} \nabla p = \nu \nabla^2 \mathbf{v} \tag{3}$$

where p is the pressure, t is the time and ρ and ν are the milk density and kinematic viscosity, respectively;

$$\frac{\partial T}{\partial t} + \mathbf{v} \cdot \nabla T = \alpha \nabla^2 T \tag{4}$$

where T is the temperature and α is the milk thermal diffusivity;

$$\frac{\partial c_i}{\partial t} + \mathbf{v} \cdot \nabla c_i = D \nabla^2 c_i \pm R_{ij} \tag{5}$$

where c_i is the molar concentration of the species i (either native *N*, denaturated *D*, aggregated *A* or deposited *F* βLG), and R_{ij} is the source term for the creation or destruction (positive rate or negative rate) reactions for each species coupling.

2.3. Initial and boundary conditions

The inlet velocity is such that the channel *Re* is 1700, 2700 or 3700 (to allow for a fluid regime sensitivity analysis); the fluid enters the channel at 60 °C with a native βLG mass concentration of 5 g/l; the auxiliary flow is counter-current saturated vapor at constant 97 °C. No-slip is enforced at every solid surface and continuity boundary conditions for heat and mass transfer have been applied to each of the internal surface.

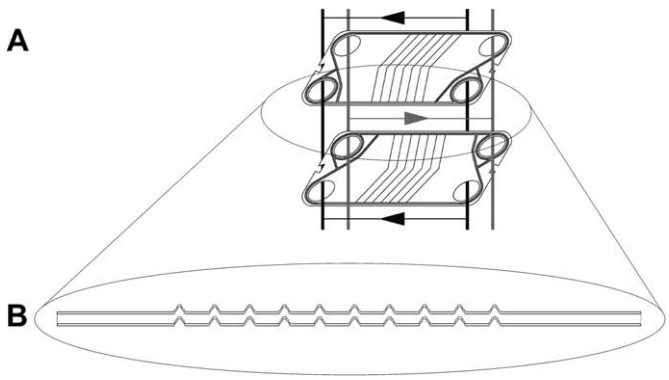

Fig. 2. The PHE's selected channel: a sector of PHE depicted in Fig. 1 (A); the close-up of the simplified corrugate plate channel (B).

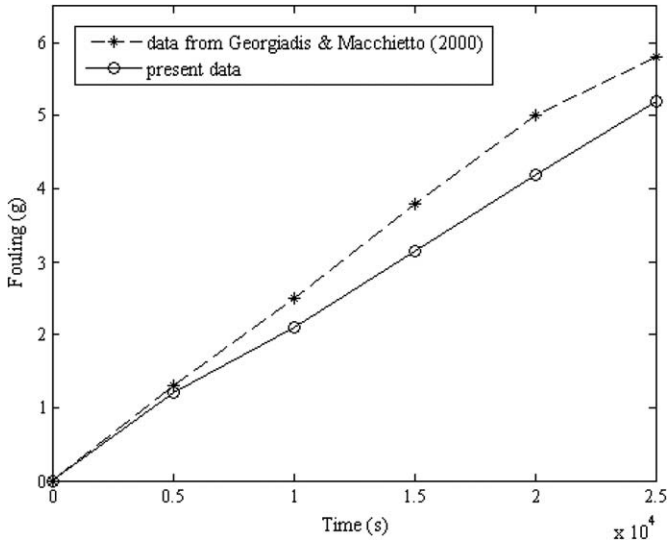

Fig. 3. Model validation: deposit profiles comparison with Georgiadis and Macchietto [4] data.

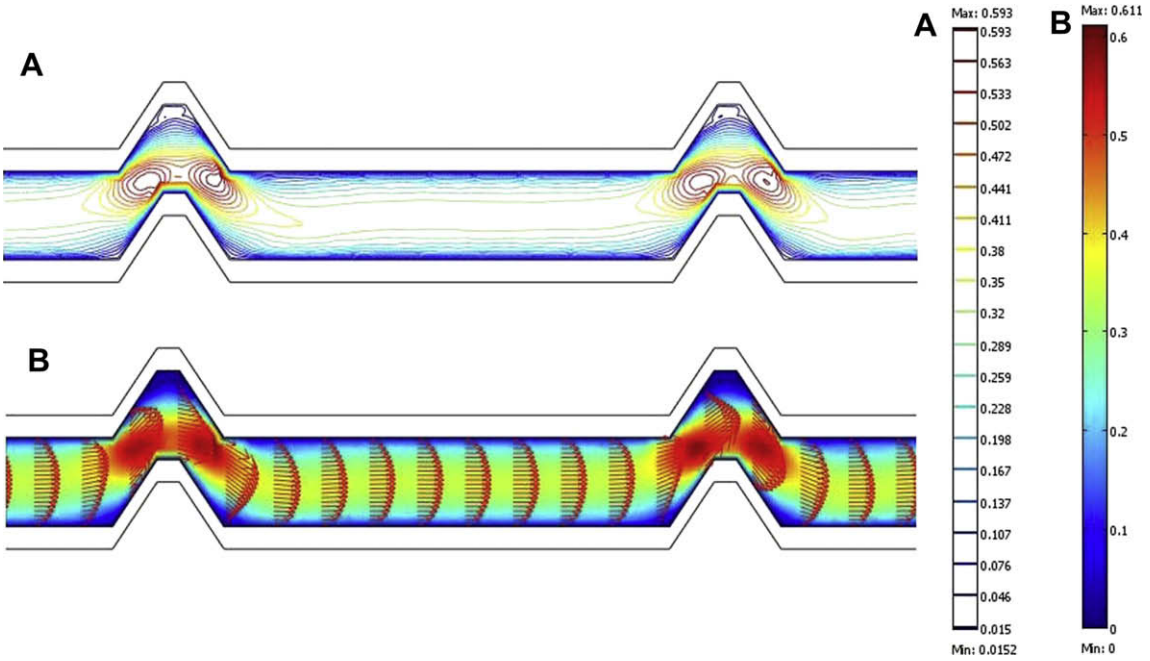

Fig. 4. Streamlines (A) and **v** (B) distribution (in the 0–0.6 m/s range) in the channel's central part, for $Re = 2700$.

2.4. An optimized kinetics approach

A mass transfer mechanism is adopted from the reference paper [7], but a modification is introduced in that two reaction types r are computed instead considering two distinct regions: a volumetric one v, and a superficial one s. Eq. (5) is substituted by the following summarizing form:

$$\frac{\partial c_{ir}}{\partial t} + \mathbf{v}\cdot\nabla c_{ir} = D\nabla^2 c_{ir} \pm R_{ij,r} \tag{6}$$

with

$$R_{ij,r} = K_r c_{ir} - K_i \Delta^{v-s} c_{ir} \pm K_s c_{As} \tag{7}$$

Here $\Delta^{v-s} c_{ir}$ is the difference between the values of volumetric and superficial concentrations, for each species; K_r's are the specific reaction rates in terms of Arrhenius expressions as in de Jong et al. [12]; and K_i and K_s are kinetics coefficients for each species and for the wall reaction rate constant for the aggregated protein on the surface of PHE, respectively. The last term at the RHS is zero for all species except for the aggregated A and fouling F proteins.

An optimization procedure was carried forth, for both volumetric and superficial reactions, by exploiting a SIMPLEX multi-object optimization. To this end, an optimization and design environment modeFRONTIER [14] was employed in which the FE code was iteratively run. This allowed optimized validations (minimizing the sum of squared differences between computations

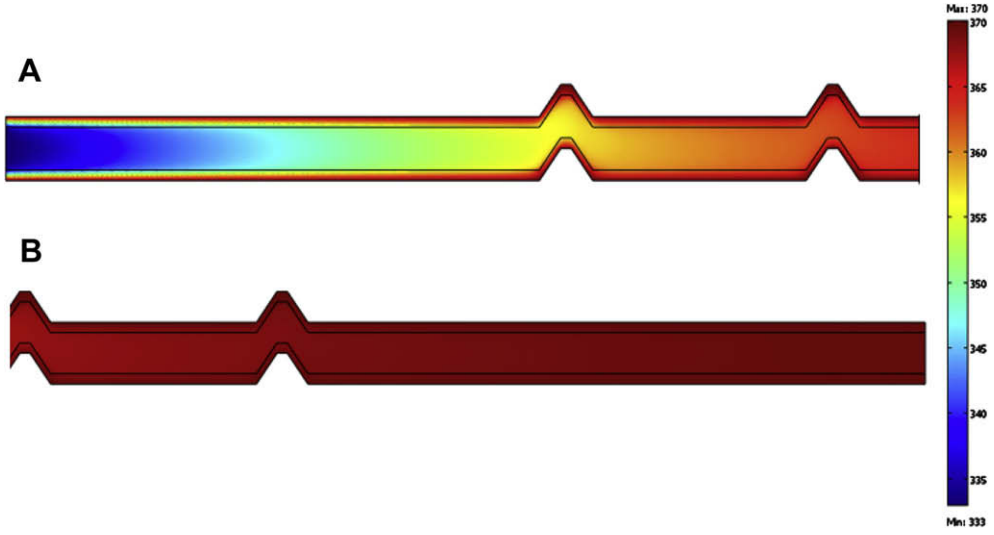

Fig. 5. T distribution (in the 330–370 K range) at the channel's inlet (A) and outlet (B) sections.

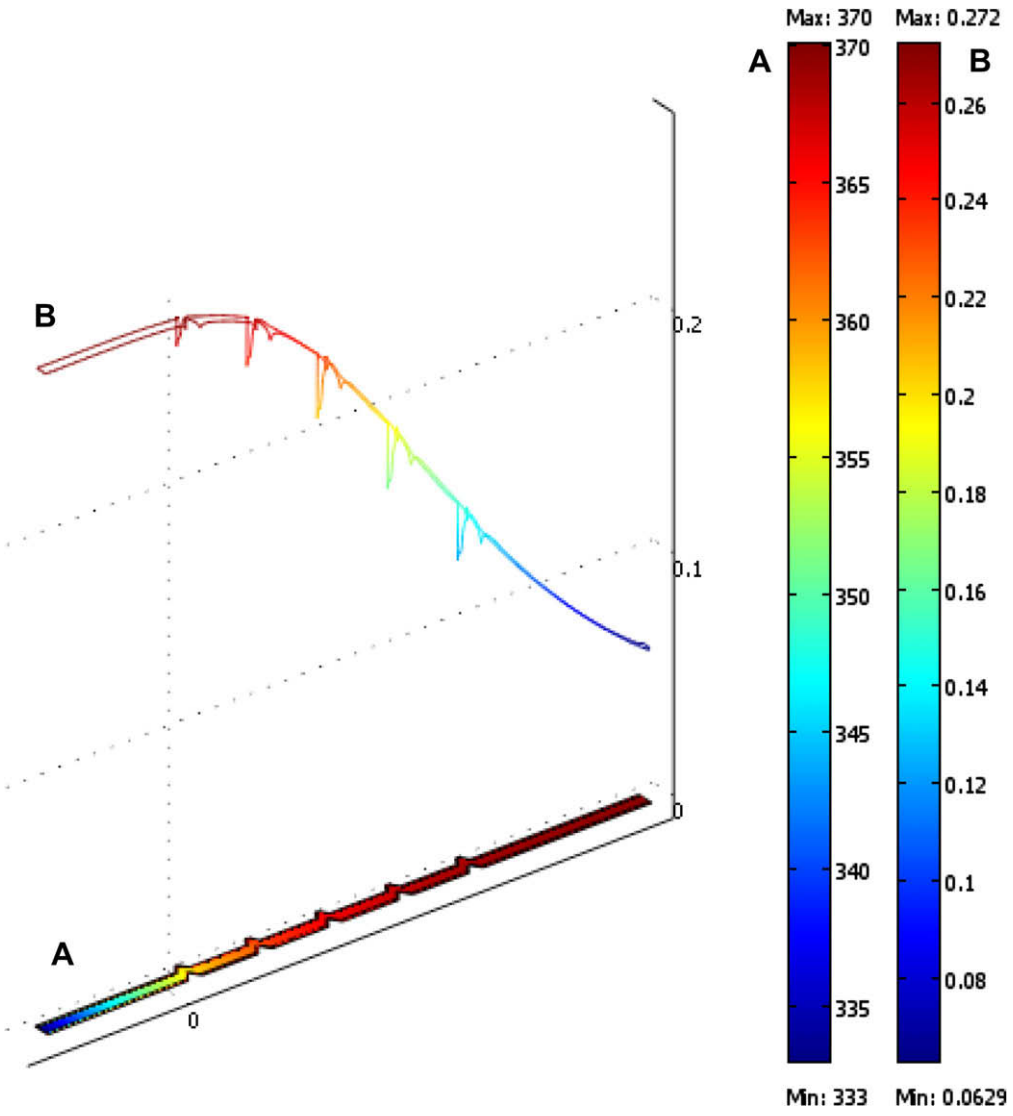

Fig. 6. Effect of T (in the 330–370 K range) (A) on c_N distribution (in the 0–0.28 mol/m^3 range) (B).

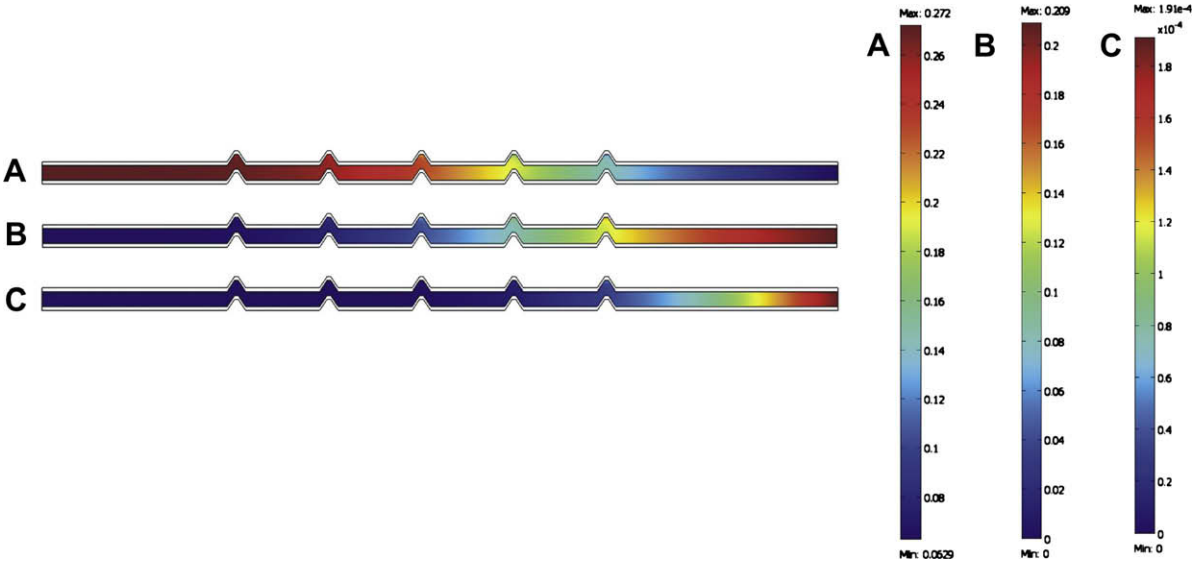

Fig. 7. c_N (A, in the 0.06–0.27 mol/m^3 range), c_D (B, in the 0–0.21 mol/m^3 range) and c_A (C, in the 0–2.0 $\times$ 10^{-4} mol/m^3 range) distributions along the channel.

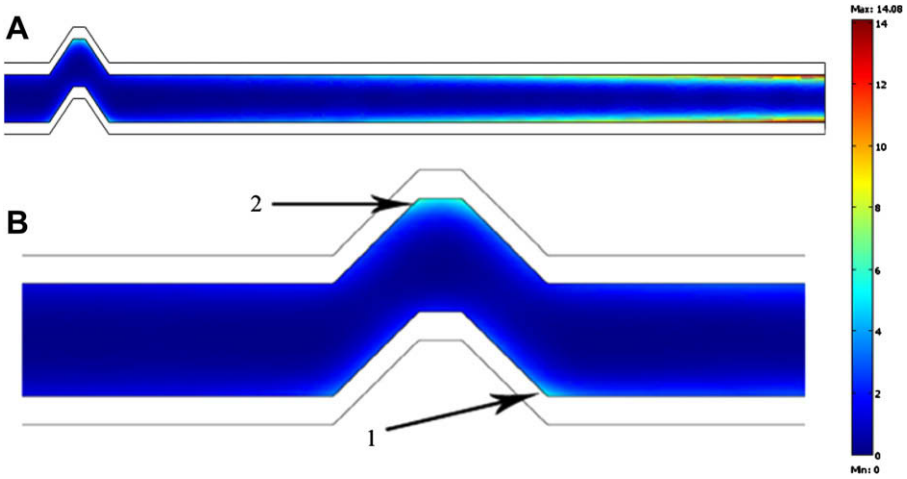

Fig. 8. c_F distribution at outlet (A) and a close-up near the last corrugation (B), with deposition loci 1 and 2 (in the 0–14 mol/m^3 range).

and literature data) with respect to transient fluid and sample average fouling concentrations.

3. Results

3.1. Numerical method, validation and additional considerations

The problem has been attacked by a grid of over 5400 finite elements and a Lagrange-Quadratic shape function [13], for a total of over 71,400 degrees of freedom. The number of mesh elements and shape function type determine the accuracy of the final solution and the solver speed. The large number of degrees of freedom is justified by the nine differential equations to be simultaneously integrated in space and advanced in time. A grid-independency analysis was not possible due to the instability of the solver for this study. The run has taken under 5 min of computing time for an elapsed time of 15 h simulation, on a Xeon server (3 GHz CPU, 2 GB RAM) running under Windows XPPro.

The model was validated by comparing the computations versus data from Georgiadis and Macchietto [4] for the average fouling deposition at $Re = 2700$ (Fig. 3). Fouling is linearly dependent with time, the agreement with literature data being fairly good, with a slight underestimation only.

3.2. Fluid flow and heat transfer

Velocity and temperature distributions help understand the fouling distribution: the flow field is reported, as streamlines and vector velocity distribution in Fig. 4A and B, respectively. Fluid acceleration is caused by the corrugations, and small stagnation regions are evident downwind from extruding corrugations and in the corresponding vanes, along all of the channel length. Fig. 5A shows the related temperature distribution at channel inlet, in the flow and in the confining plates. Temperature readily changes from its initial value of 60 °C in milk, while the walls are being cooled-off by the fresh fluid, whereas at channel outlet, in Fig. 5B, due to the combined heating by the channel walls and streamwise convection, the temperature is finally uniform at 97 °C.

3.3. Mass transfer

The thermal damage is initiated in those regions where the fluid is slowed down and the contact time with heating walls is longer. In Fig. 6A the temperature increase is clearly correlated to the depletion of βLG_N in Fig. 6B, at channel outlet where the temperature is highest. The βLG_N is also locally depleted due to the aforementioned flow pattern: the fluid can remain in contact with the plate for a long time in the stagnant zones created in every superior vane.

The relationship between the three *N*, *D* and *A* proteins can be discussed by comparing their concentration maps in Fig. 7A, B and C, respectively. At channel's inlet, with a relatively low temperature, *N* is at its initial value and neither *D* nor *A* are detected. Along the channel, however, *D* and *A* concentrations depend on temperature evolution and begin to increase, c_D increasing faster (and complementarily to *N*) than c_A. In particular, c_A distribution is informative on the aggregation progress that occurs in the channel, and it forms almost exclusively towards the outlet. This different behavior can be attributed to the additional K_s term, that works in the model as a deposition kinetic term and therefore directly drives the fouling process, being referred to *A* and *F* proteins only.

Moreover, Fig. 8 speculates on the topology of the deposition. It is seen that the most of the fouling is created in the outlet section of the channel, where the c_A concentration is denser (Fig. 8A), while some specific deposition loci appear also downwind of last

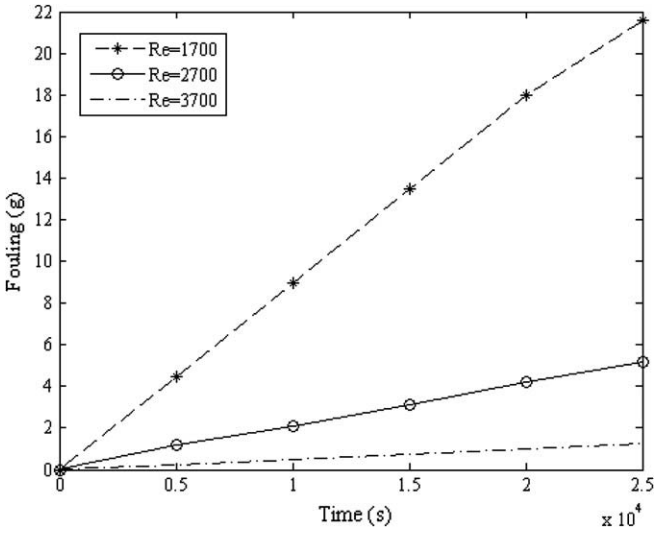

Fig. 9. Deposition for different *Re*.

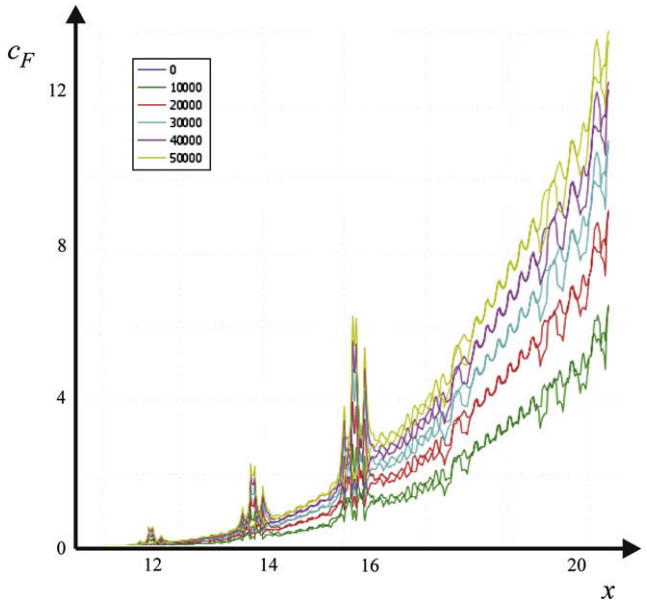

Fig. 10. c_F evolution (in the 0–14 mol/m^3 range) along the channel axis x, at the last three corrugations and in the final channel section, during a 14 h period (5 time intervals of 10^4 s).

corrugation (1), as well as its corresponding vane (2) (Fig. 8B), where the small stagnation regions are found (as in Fig. 4A).

The effect of different fluid regimes is then presented in Fig 9. Protein fouling depends inversely on *Re*, with the highest accumulation level of 22 g after about 7 h of operation (when $Re = 1700$). It is evident that the coupling between momentum, heat and mass transfer is such that the deposition is nonlinearly dependent on the velocity decrement: when the average inlet velocity is doubled, the fouling decreases more than 10 times.

Finally, the fouling's time evolution of fouling along the channel is reported in Fig. 10, for a 14 h duration process. The formation of the deposited protein is nonlinear with time, as accretion rate decreases; after the first 20,000 s (about 5.5 h) the fouling formation is fastest, but during the second 30,000 s (8.3 h) period the deposition slows down.

Some studies have been found in the available literature on the optimization of periodic channels [8,10], with the aim of heat transfer rate maximization and friction factor minimization. A similar approach could be exploited, based on the present model, to modify the channel geometry, when this is parameterized by means of non-uniform rational b-splines, but imposing biochemical conditions instead, that could allow for different corrugation shapes depending on the specific working fluid. In this way, by using the present approach, plate profiles could be studied to lengthen the working cycles affected by protein, enzyme and microbial kinetics interaction with heat and fluid flow.

4. Conclusions

CFD modeling can prove useful in product, process and system design, and in real-world problem resolution in the food and biotech industry. In this work the fouling by βLG has been described by integrating a governing PDEs set when modeling a corrugated-plate heat exchanger during pasteurization of milk. Fouling formation is strictly dependent upon the wall temperature distribution, but also on local flow deceleration that favor solid deposition by inhibiting fluid abrasion and increasing wall temperature. Local species concentration, velocity and temperature can be ascertain to test new corrugation shapes and orientations, to minimize fouling. In this way, innovative configurations and designs can be inferred and proposed.

References

[1] R.T. Bott, Fouling of Heat Exchangers, Elsevier Science & Technology Books, New York, 1995.
[2] H. Burton, Ultra-high Temperture Processing of Milk and Milk Products, Elsevier Applied Science, London, 1988.
[3] M.C. Georgiadis, G.E. Rotstein, S. Macchietto, Modelling and simulation of complex plate heat exchanger arrangements under milk fouling, Computers Chemical Engineering 22 (1998) 331–338.
[4] M.C. Georgiadis, S. Macchietto, Dynamic modelling and simulation of plate heat exchangers under milk fouling, Chemical Engineering Science 55 (2000) 1605–1619.
[5] K. Grijspeerdt, L. Mortier, J. De Block, R. Van Renterghem, Application of modelling to optimise ultra high temperature milk heat exchangers with respect to fouling, Food Control 15 (2004) 117–130.
[6] S. Jun, V.M. Puri, Fouling models for heat exchangers in dairy processing: a review, Journal of Food Process Engineering 28 (2004) 1–34.
[7] S. Jun, V.M. Puri, A 2D dynamic model for fouling performance of plate heat exchangers, Journal of Food Engineering 75 (2006) 364–374.
[8] M. Manzan, E. Nobile, S. Pieri, F. Pinto, Multiobjective optimization for problems involving convective heat transfer, in: D. Thevenin, G. Janiga (Eds.), Optimization based on Computational Fluid Dynamics, Springer, New York, 2008, pp. 217–266.
[9] P.K. Nema, A.K. Datta, Improved milk fouling simulation in a helical triple tube heat exchanger, International Journal of Heat and Mass Transfer 49 (2006) 3360–3370.
[10] E. Nobile, F. Pinto, G. Rizzetto, Geometrical parameterization and multi-objective shape optimization of convective periodic channels, Numerical Heat Transfer, Part B 50 (2006) 425–453.
[11] R.K. Shah, E.C. Subbarao, R.A. Mashelkar, Heat Transfer Equipment Design, Hemisphere Publishing Corporation, Washington, 1988.
[12] P. de Jong, S. Bouman, H.J.L.J. Van der Linden, Fouling of heat treatment equipment in relation to the denaturation of β–lactoglobulin, Journal of the Society of Dairy Technology 45 (1992) 3–8.
[13] COMSOL Multiphysics User's Guide, COMSOLAB, 2007.
[14] ModeFRONTIER User's Guide, ES.TECO. srl, 2007, (sold by Enginsoft srl).